Seeing is Simulating: Differentiable Physics for Interaction-Aware Material Estimation

Anonymous authors
Paper under double-blind review

Abstract

Modeling human-object interactions is crucial for creating immersive virtual experiences. However, synthesizing 3D object dynamics conditioned on actions remains a challenging problem. Existing approaches equip static 3D objects with motion priors distilled from video diffusion models. However, this methodology has two drawbacks: (i) video diffusion models are not physically grounded. Thus, the generated videos may contain physical inaccuracies; (ii) video diffusion models cannot generate complex dynamics where multiple objects interact under actions with long durations and large spatial extent. We present **PhysInteract**, a physics-based framework that (i) models interactions with a representation that captures their duration and contact information; (ii) estimates object material properties (e.g., Young's modulus) from objects' deformation caused by interactions; (iii) uses physics simulation to reproduce realistic object dynamics based on estimated interactions and material properties. We highlight that PhysInteract is fully differentiable, enabling joint optimization of interaction representations and object material properties. PhysInteract achieves better performance than existing methods Zhang et al. (2024); Xie et al. (2024a). We demonstrate its superiority by quantitatively testing PhysInteract on a curated dataset. In conjunction with an additional user study, our method shows a step towards more realistic and immersive virtual experiences.
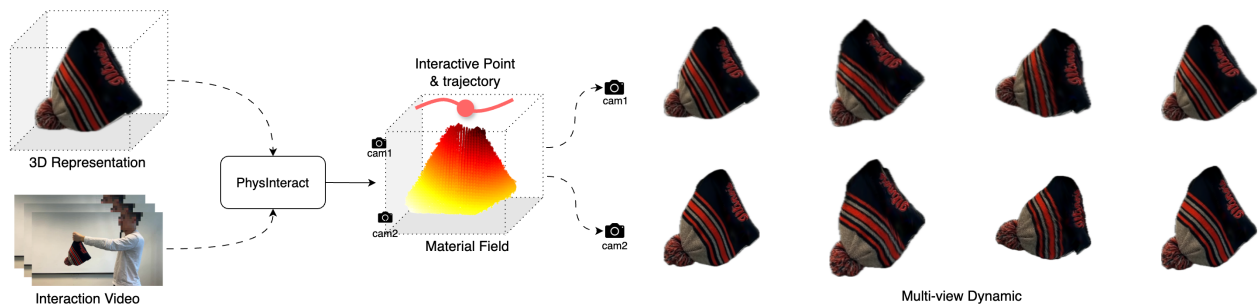

Figure 1: PhysInteract is designed to model human-object dynamics. Given an objects 3D representation and a video depicting interactions with the object, it first models interactions using the trajectories of a set of interactive points, then estimates the object's material properties (e.g., Youngs modulus), and finally uses physics simulation to reproduce the realistic object dynamics shown in the input video.

1 Introduction

Modeling human-object interactions is a pivotal component in creating immersive virtual experiences. It requires not only the ability to interpret interactions in the wild but also the capacity to synthesize physically plausible deformations of objects in response to these actions. However, achieving this remains a formidable challenge due to two primary factors: **(i)** Complexity of Interaction Modeling. Interactions are

temporal events involving multiple entities, such as duration, contact points, and force trajectories. Accurately identifying them from unstructured video data is difficult. Furthermore, translating these abstract concepts into structured representations compatible with physics simulations poses a significant hurdle; **(ii)** Requirement for Causal Physical Understanding. Entities in an interaction undergo continuous state changes. For instance, velocities and poses are altered by external forces, and non-rigid objects deform upon contact. Capturing these causal relationships is essential for the accurate modeling of human-object interactions, yet it requires reasoning beyond simple visual correspondence.

Prior work has predominantly used statistical methods to address these challenges. Leveraging the generative power of diffusion models, several approaches Chen et al. (2024b); Li et al. (2024); Zhang et al. (2023); Ren et al. (2023); Zhao et al. (2023) animate still images or 3D assets based on user inputs, such as text prompts or direct manipulation (e.g., dragging). While these methods yield visually compelling results, they are generally not physically grounded. Consequently, artifacts and physically impossible distortions are frequently observed. To mitigate this, recent research has incorporated explicit physics priors. Methods like Xie et al. (2024a); Zhang et al. (2024) utilize the Material Point Method (MPM) Jiang et al. (2016) to simulate 3D dynamics based on material properties derived from video motion priors. However, these approaches often rely on an oversimplified assumption where object motion is driven by inertia from an initial velocity. They lack a mechanism to model continuous, external human-object interactions, rendering them incapable of handling complex dynamics in which objects are subjected to sustained actions over long durations and extensive spatial contact.

To bridge this gap, we propose *PhysInteract*, a fully differentiable, physics-based framework designed to accurately model human-object interactions. Taking a 3D representation (e.g., Gaussian Splatting Kerbl et al. (2023) or mesh) and a monocular video depicting the interaction as input, PhysInteract operates through three integrated stages: **(i)** Interaction Representation Construction. Instead of relying on simple initial states, PhysInteract explicitly models the interaction trajectory. By leveraging vision-language models and segmentation tools (e.g., SAM Ravi et al. (2024)) to localize contact areas, we back-project these regions into 3D space as "contact points". We then track these "contact points" over time to construct a coarse interaction trajectory that drives the object's deformation; **(ii)** Differentiable Physics Simulation. We employ a differentiable MPM simulator to model 3D dynamics. This simulator requires intrinsic material propertiessuch as Young's modulus (stiffness) and Poisson's ratio (deformability), which are initially unknown. PhysInteract initializes these parameters randomly or via heuristics; **(iii)** Joint Optimization. A core innovation of PhysInteract is the joint optimization of interaction representations and material properties. Since the initially extracted trajectories may be inaccurate, simply optimizing material properties leads to suboptimal solutions. Therefore, PhysInteract iteratively refines both the contact point trajectories (forces) and the object's material parameters by minimizing the discrepancy between the rendered simulation and the original video frames. This "analysis-by-synthesis" loop allows us to recover accurate physical parameters and realistic motion simultaneously.

To evaluate our method, we curate a dataset featuring objects with diverse material properties (e.g., elastic rubber, jelly) undergoing various interactions (e.g., pulling, dragging). Quantitative experiments demonstrate that PhysInteract significantly outperforms existing approaches in modeling fidelity. Furthermore, extensive user studies validate our method's superiority in motion realism and visual quality. Notably, PhysInteract exhibits strong generalization capabilities: once material properties are estimated, the system can generate realistic object dynamics conditioned on novel, unseen interactions without retraining.

To summarize, our contributions are threefold:

- We propose a novel framework, PhysInteract, that accurately models human-object interactions by jointly estimating interaction trajectories and material properties within a unified, differentiable optimization process.

- We introduce a comprehensive dataset containing diverse human-object interaction samples to facilitate future research in this domain.

- We conduct extensive experiments and user studies, demonstrating state-of-the-art visual quality and the ability to synthesize dynamics conditioned on novel interactions.

2 Related Work

4D content generation. This field aims to synthesize 4D representations that maintain both multi-view and temporal consistency. A prevalent paradigm involves integrating 3D generation pipelines with video diffusion models. For instance, Xie et al. (2024b); Bahmani et al. (2024); Yin et al. (2023); Ling et al. (2024); Zhao et al. (2023); Jiang et al. (2023); Chen et al. (2024a); Ren et al. (2023); Singer et al. (2023); Zeng et al. (2024); Yang et al. (2024) extend static 3D representations to the temporal dimension via Score Distillation Sampling loss Poole et al. (2022). While yielding plausible visual results, these methods inherently struggle with the high computational cost and instability associated with SDS and video diffusion models. Furthermore, due to the hallucination problem characteristic of generative models Radford et al. (2018), they often fail to ensure accurate multi-view consistency or kinematic plausibility. Alternatively, geometry-based methods Pan et al. (2024); Sun et al. (2024); Kratimenos et al. (2024); Duan et al. (2024); Das et al. (2024); Liang et al. (2025); Lin et al. (2024) adapt 3D reconstruction pipelines to 4D content by utilizing multi-view images at every timestep. Although these approaches offer superior optimization efficiency, their applicability is severely constrained by the scarcity of high-quality, synchronized multi-view 4D data, limiting their generalization potential.

In contrast, PhysInteract generates plausible 4D content using only monocular videos. By integrating a forward-pass simulation engine, we ensure strict physicality and temporal consistency without relying on computationally intensive generative priors.

Simulation-based generation. To enhance physical realism, recent works Feng et al. (2024); Li et al. (2023); Xie et al. (2024a) impart physical properties to 3D representations, endowing them with kinematic attributes (e.g., velocity, strain) and mechanical properties (e.g., stiffness, plasticity). These representations are then driven by the laws of continuum mechanics to produce 4D dynamics. A central challenge in this domain is obtaining the accurate physical parameters required for simulation. Early approaches Tan et al. (2024); Xie et al. (2024a); Zhao et al. (2024); Lin et al. (2025) derive such knowledge from human priors or Large Language Models (LLMs). However, these methods often suffer from a domain gap between semantic descriptions and precise physical coefficients, resulting in inaccuracies. Consequently, recent efforts have shifted towards optimization-based parameter estimation. For example, Zhang et al. (2024); Huang et al. (2025); Liu et al. (2024a) distill dynamic priors from video generation models. However, as discussed in Section 1, these methods predominantly focus on inertial motion initiated by an initial state, lacking the capability to model complex scenarios involving continuous, external human-object interactions. Moreover, relying on generative video priors can introduce accumulated errors in physical parameter estimation.

In this work, we address these limitations by learning directly from real-world interactions. PhysInteract jointly optimizes interaction forces and material properties, ensuring that the synthesized dynamics are grounded in accurate, real-world physical observations.

3 Method

Overview. Given a monocular video capturing an object undergoing interaction-driven motion, along with its static 3D representation (e.g., 3D Gaussians Kerbl et al. (2023) or mesh), our goal is to jointly estimate the object's physical material properties (e.g., Young's modulus) and the precise interaction dynamics (e.g., contact forces/trajectories). As illustrated in Figure 2, PhysInteract operates in three stages: **(1)** Initialization. We first leverage vision-language and tracking models to construct a coarse representation of the interaction (Section 3.2); **(2)** Joint Optimization. We employ a differentiable physics simulator to iteratively refine both the material properties and the interaction trajectory by minimizing the discrepancy between simulated renderings and observed video frames (Section 3.3); **(3)** Inference. Finally, the learned physical model enables the synthesis of realistic dynamics conditioned on novel interactions (Section 3.4).

3.1 Preliminaries

3D representation. We adopt 3D Gaussian Splatting (3DGS) Kerbl et al. (2023) as our primary representation due to its explicit Lagrangian nature, which is naturally compatible with particle-based physics
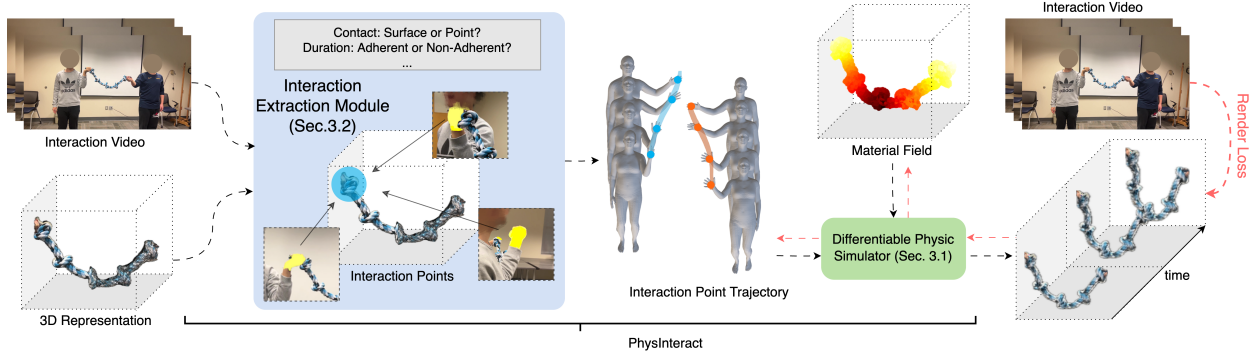
Figure 2: Overview of PhysInteract. Given an interaction video and a static 3D representation, our framework jointly estimates the physical material properties and interaction dynamics. The Interaction Extraction Module (Section 3.2) first leverages vision-language models to infer interaction semantics (e.g., contact type) and employs grounding models (Segment Anything Model Ravi et al. (2024)) to localize 3D contact points. This initializes a coarse Interaction Point Trajectory. This trajectory, along with a learnable Material Field (representing per-particle Young's modulus), is fed into a Differentiable Physics Simulator (Section 3.1). Through an analysis-by-synthesis loop, we compute a Render Loss between the simulated 4D dynamics and the observed video frames. As indicated by the red dashed arrows, gradients are back-propagated to jointly optimize both the material field and the interaction trajectory (Section 3.3), ensuring physically plausible motion reconstruction.

simulators. The object is parameterized as a set of Gaussians $\{\mathcal{G}_p\}_{p=1}^P$, where each particle $\mathcal{G}_p$ possesses position $\boldsymbol{x}_p$, covariance Σ_p, opacity α_p, and color $\boldsymbol{c}_p$. While we focus on 3DGS, our framework is agnostic and also compatible with mesh-based representations.

Differentiable material point method. To simulate physically grounded motion, we utilize the Material Point Method (MPM) Jiang et al. (2016), a hybrid Lagrangian-Eulerian solver. The simulation follows the laws of continuum mechanics, governed by the conservation of mass and momentum. The object's deformation is characterized by the deformation gradient $\boldsymbol{F}$, and the internal stress σ is computed via a constitutive model. We employ the Fixed Corotated elasticity model, where the stress-strain relationship is defined by the energy density function $\psi(\boldsymbol{F})$:

$$\psi(\boldsymbol{F}) = \mu \sum_{i=1}^d (\sigma_i - 1)^2 + \frac{\lambda}{2}(\det(\boldsymbol{F}) - 1)^2, \tag{1}$$

Here, σ_i are the singular values of $\boldsymbol{F}$. The Lamé parameters μ and λ are derived from the object's material properties: Young's modulus E (stiffness) and Poisson's ratio ν (compressibility). Crucially, our MPM simulator is *fully differentiable*. This allows gradients to propagate from the rendered image loss back through the simulation steps to update both the initial material parameters (E, ν) and the external interaction forces.

3.2 Initialization: Interaction Representation

Directly optimizing physics parameters from scratch is prone to local minima. Therefore, we propose a multi-stage initialization strategy to construct a coarse but semantically meaningful interaction representation.

Semantic parsing via vision language models. We first employ a Vision-Language Model (VLM) Bai et al. (2023) to parse the video context. The VLM identifies: (i) interaction type (e.g., point-based contact vs. surface collision); and (ii) temporal characteristics (e.g., continuous grasping vs. instantaneous impact). This semantic prior guides the subsequent geometric extraction.

Contact point localization. To locate the physical contact, we utilize an open-vocabulary grounding model Liu et al. (2024b) to detect the interaction region (e.g., "hand") bounding box $\mathbf{B}$, followed by the

Segment Anything Model (SAM) Ravi et al. (2024) to extract a precise 2D contact mask M_{contact}. To lift this 2D information into 3D, we estimate the camera pose $\mathbf{T}_c$ and object pose $\mathbf{T}_o$ via differentiable rendering alignment (optimizing RGB and silhouette consistency). We then back-project the masked pixels $\mathbf{x}_p \in M_{\text{contact}}$ into 3D space using the estimated depth d_p:

$$\mathbf{X}_p = (\mathbf{T}_c)^{-1} \pi^{-1}(\mathbf{x}_p, d_p). \tag{2}$$

This yields a set of 3D particles $\mathcal{P}_{\text{contact}}$ representing the interaction interface. This process is similar to that described in Yang et al. (2021).

Trajectory initialization. An interaction is defined not just by contact, but by motion. We initialize the interaction trajectory $\mathcal{T}^{(0)}$ based on the scenario: for human-object interaction, we lift 2D tracks from a human pose tracker (e.g., 4D Humans Goel et al. (2023)) to 3D; for object-object interaction, we utilize scene flow tracking Wang et al. (2025). This initial trajectory $\mathcal{T}^{(0)}$ serves as a "soft guide" for the subsequent physics-based optimization.

3.3 Physics-Aware Joint Optimization

The initialization described above relies on visual observations, which effectively capture kinematics but lack physical causality. Therefore, we propose a joint optimization framework that refines both the interaction dynamics and the material properties through an analysis-by-synthesis loop.

Parameterization. We optimize two sets of parameters:

- **Material Field** Θ_{mat}: We parameterize the physical properties explicitly on the particles. Specifically, we assign a Young's modulus E_p and a Poisson's ratio ν_p to each particle p (including both surface Gaussians and internal filling particles). This enables the representation of spatially varying material properties that naturally deform with object geometry.

- **Interaction Trajectory** $\mathcal{T}$: We parameterize the interaction as a sequence of velocity boundary conditions or external forces $\{\mathbf{f}_t\}_{t=1}^T$ applied to the contact particles $\mathcal{P}_{\text{contact}}$.

Forward simulation and rendering. At each optimization step, the simulator takes the current material field Θ_{mat} and interaction $\mathcal{T}$ to simulate the object's dynamics from $t = 0$ to $t = T$, producing a sequence of deformed particle states $\{\mathbf{x}_t\}_{t=1}^T$. These states are then rendered into images $\{\hat{I}_t\}_{t=1}^T$ via a differentiable Gaussian splatting renderer proposed in Kerbl et al. (2023).

Objective function. We optimize Θ_{mat} and $\mathcal{T}$ jointly by minimizing a composite loss function:

$$\mathcal{L}_{\text{total}} = \mathcal{L}_{\text{rec}} + \lambda_{\text{reg}} \cdot \mathcal{L}_{\text{reg}}. \tag{3}$$

The reconstruction loss $\mathcal{L}_{\text{rec}}$ enforces visual fidelity:

$$\mathcal{L}_{\text{rec}} = \sum_t \left(\|\hat{I}_t - I_t\|_1 + \lambda_{\text{ssim}}(1 - \text{SSIM}(\hat{I}_t, I_t)) + \lambda_{\text{mask}}\|\hat{M}_t - M_t\|_2 \right), \tag{4}$$

where I_t, M_t are ground-truth video frames and silhouettes. To ensure physical plausibility and prevent overfitting to visual noise, we apply regularization $\mathcal{L}_{\text{reg}}$:

$$\mathcal{L}_{\text{reg}} = \|\nabla\Theta_{\text{mat}}\|_2 + \|\mathcal{T} - \mathcal{T}^{(0)}\|_2, \tag{5}$$

which encourages spatial smoothness in the material field and constrains the optimized trajectory to remain semantically consistent with the visual initialization $\mathcal{T}^{(0)}$.

Table 1: Dataset details. We evaluate PhysInteract on 11 scenes comprising diverse object types (Synthetic and Real) and multiple interaction modalities.

Scene	Source	Object	Interaction Type
1	Sync	Hemp rope	Point Adherent
2	Sync	Bow tie	Point Adherent
3	Sync	Tow rope	Point Adherent
4	Sync	Glove	Point Adherent
5	Sync	Balloon Dog	Point Adherent
6	Sync	Basketball	Surface Non-Adherent
7	Sync	Balloon	Point Adherent
8	Sync	Flower	Point Adherent
9	Real	Knit cap	Point Adherent
10	Real	Telephone cable	Point Non-Adherent
11	Real	Toy rope	Point Adherent

3.4 Inference: Novel Interaction Synthesis

Once the optimization converges, we obtain a physically calibrated representation of the object, encapsulated in the estimated material field Θ^*_{mat}, which allows PhysInteract to generalize. We can now discard the original interaction $\mathcal{T}$ and apply novel, user-defined interactions $\mathcal{T}_{\text{new}}$ (e.g., applying a new force at a different location). By running the forward MPM simulation with Θ^*_{mat} and $\mathcal{T}_{\text{new}}$, we synthesize realistic 4D dynamics that are not present in the original video, enabling applications such as interactive virtual editing.

3.5 Implementation Details

Internal filling. Standard 3DGS representations only model the object surface, whereas physics simulations require a continuum volume. To address this, we implement an internal filling strategy. For mesh inputs, we perform voxelization. For Gaussian inputs, we first densify particles within the Gaussian ellipsoids to approximate local volume, and then apply voxel-based filling to populate the interior. These internal particles are assigned the same material properties as their nearest surface neighbors and participate in the MPM simulation to ensure structural stability.

Training details. We implement PhysInteract using PyTorch and the Taichi programming language Hu (2018) for differentiable MPM simulation. The optimization is performed on a single NVIDIA A40 GPU. We use the AdamW optimizer Loshchilov & Hutter (2017) for both material properties and interaction trajectories. The learning rates are initialized at 1×10^{-4} for material parameters and 5×10^{-5} for trajectory updates, with a cosine annealing schedule. The optimization typically converges within $5,000$ iterations, taking approximately 30 minutes per video sequence.

4 Experiments

4.1 Experimental setup

Dataset. Due to the scarcity of high-quality 4D interaction data with ground truth physical properties, we curated a hybrid dataset comprising both synthetic and real-world scenes. As detailed in Table 1, our dataset consists of 11 diverse scenes covering: **(1)** Synthetic Scenes (8 sequences): we simulated objects with varying geometries (e.g., hemp rope, bow tie, balloon dog) and material properties using accurate physics engines, which provides ground truth for quantitative physical evaluation. **(2)** Real-world Scenes (3 sequences): we captured real-world interactions involving a telephone cable, a knit cap, and a toy rope. Crucially, the dataset spans multiple interaction types, including "Point Adherent" (e.g., grasping), "Point Non-Adherent" (e.g., poking), and "Surface Non-Adherent" (e.g., bouncing), ensuring comprehensive robustness evaluation.

Table 2: Quantitative comparison. We report SSIM (S) and PSNR (P) across all 11 scenes. Baselines include PhysDreamer (PD), DreamGaussian4D (DG4D), and GPT+PhysGaussian (GPT-PG). Our method consistently achieves state-of-the-art reconstruction quality.

Method	Scene 1		Scene 2		Scene 3		Scene 4		Scene 5		Scene 6	
	S	P	S	P	S	P	S	P	S	P	S	P
PD	0.63	14.78	0.62	15.05	0.67	17.23	0.53	14.62	0.61	14.03	0.52	13.99
DG4D	0.63	14.18	0.64	15.32	0.71	17.89	0.64	14.81	0.63	14.63	0.62	14.52
GPT-PG	0.66	15.05	0.68	17.23	0.42	12.02	0.58	15.88	0.62	14.01	0.66	15.98
Ours	**0.89**	**22.38**	**0.87**	**21.37**	**0.81**	**20.75**	**0.88**	**23.71**	**0.91**	**21.94**	**0.89**	**22.56**

Method	Scene 7		Scene 8		Scene 9		Scene 10		Scene 11		Average	
	S	P	S	P	S	P	S	P	S	P	S	P
PD	0.67	16.81	0.61	15.48	0.46	14.79	0.49	9.33	0.64	12.70	0.58	14.44
DG4D	0.64	15.79	0.62	14.21	0.46	13.80	0.54	9.96	0.51	10.87	0.60	14.18
GPT-PG	0.68	16.01	0.61	15.89	0.51	14.21	0.50	13.34	0.57	11.01	0.59	14.60
Ours	**0.75**	**20.63**	**0.94**	**23.94**	**0.73**	**20.65**	**0.71**	**19.5**	**0.94**	**24.92**	**0.84**	**22.03**

Implementation details. We leverage a vision-language model Bai et al. (2023) to analyze visual content and infer interaction types by framing the prompt as a multiple-choice question. Following this, we employ SAM Ravi et al. (2024) to segment interaction regions. For human-object scenarios, 4D-Humans Goel et al. (2023) is used to initialize trajectories; otherwise, we utilize scene flow tracking Wang et al. (2025). To ensure computational efficiency, we crop foreground objects into a normalized $[0.0, 3.0]^3$ space discretized by a 100^3 MPM grid. Objects are represented by approximately $5,000$ surface particles. Moreover, to guarantee simulation stability, we augment these with $5,000$ to $10,000$ internal filling particles, which share the same physical properties as surface particles but are excluded from rendering.

Baselines We compare PhysInteract against three state-of-the-art approaches. We analyze their mechanisms and limitations below:

- **PhysDreamer** Zhang et al. (2024): estimates physical properties using video priors from diffusion models. *Limitation:* It models motion via a velocity field that only captures internal deformation. Consequently, it fails to account for external forces in interaction scenarios, leading to incorrect velocity predictions.

- **DreamGaussian4D** Ren et al. (2023): optimizes 4D Gaussians directly from video via deformation fields. *Limitation:* It lacks explicit physical modeling. As particle counts increase, the optimization landscape becomes highly complex, causing it to struggle with simultaneous large deformations and external interactions.

- **GPT + PhysGaussian** Xie et al. (2024a): adapts PhysGaussian by using GPT Achiam et al. (2023) to infer material parameters from video, which are then fed into the simulator. *Limitation:* LLMs often struggle to map visual observations to precise numerical physical coefficients (e.g., Young's Modulus), leading to plausible but physically inaccurate simulations.

4.2 Quantitative Evaluation

Visual fidelity. We first evaluate the visual quality of the reconstructed motion using the Structural Similarity Index (SSIM) Wang et al. (2004) and the Peak Signal-to-Noise Ratio (PSNR). As shown in Table 2, PhysInteract consistently outperforms all baselines across all 11 scenes. Specifically, we achieve an average PSNR of 22.03, significantly surpassing the best baseline (GPT+PhysGaussian: 14.60). This indicates that our joint optimization of physics and interaction trajectories yields the most faithful reconstruction of observed dynamics.

Results for synthetic data   Material Field

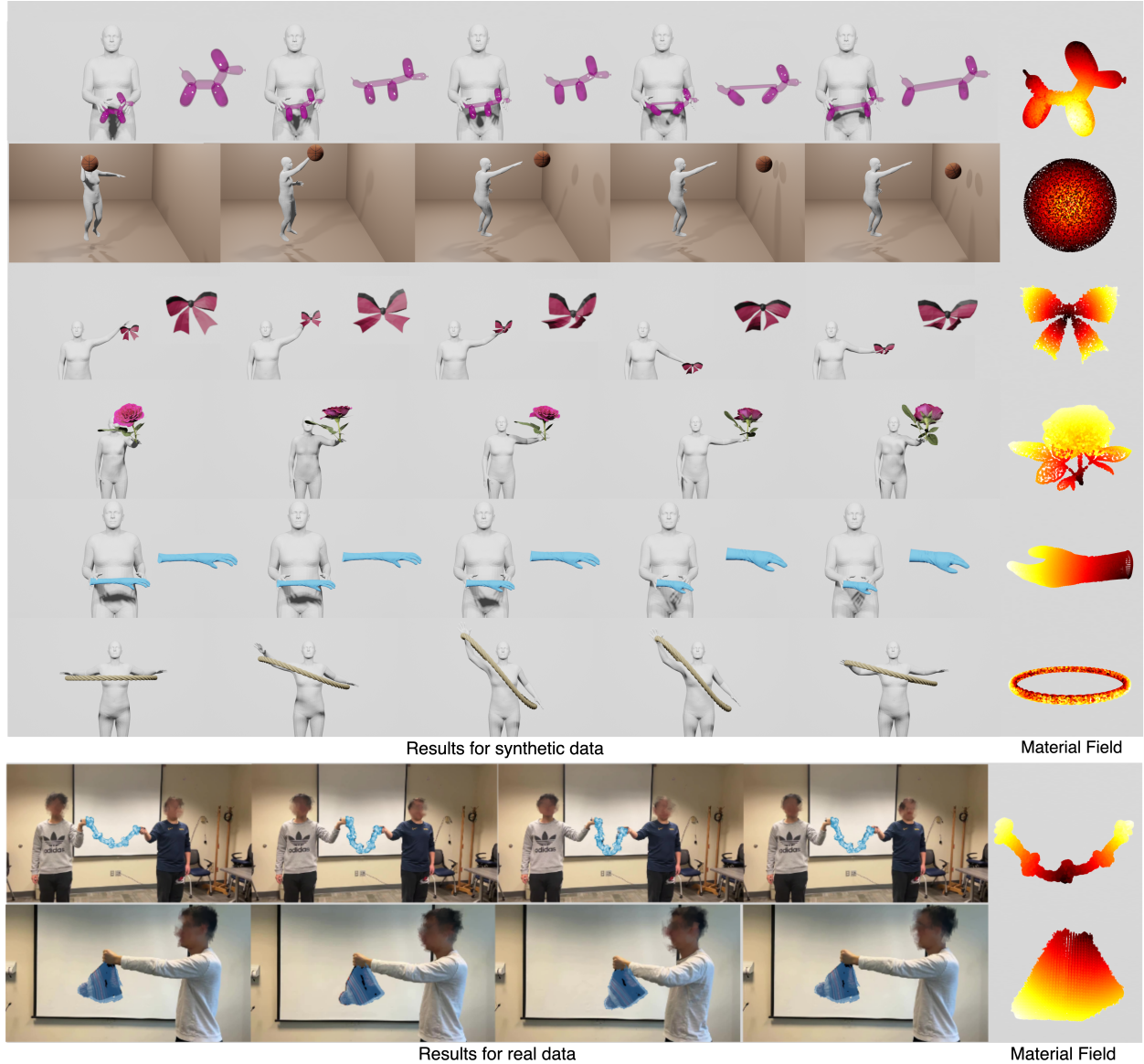Results for real data   Material Field

Figure 3: Qualitative results of PhysInteract. We visualize the reconstructed interaction sequences across diverse scenarios, including synthetic data (top three rows) and real-world captures (bottom two rows). For each sequence, we display key frames of the interaction. The rightmost column visualizes the learned material field (Young's Modulus), where warmer colors indicate higher stiffness. Our method successfully reconstructs complex deformations (e.g., balloon twisting) and interactions (e.g., rope pulling) while recovering spatially consistent physical properties.

Table 3: Material estimation accuracy. Evaluated on synthetic scenes. We compare our full model against a variant without joint trajectory optimization (*w/o JO*). The results show that refining trajectories is essential for accurate material estimation.

Method	Scene 1	Scene 2	Scene 3	Scene 4	Scene 5	Scene 6	Scene 7	Scene 8	Average
w/o JO	0.721	0.685	0.654	0.782	0.710	0.745	0.690	0.805	0.724
Ours	**0.853**	**0.812**	**0.794**	**0.887**	**0.823**	**0.861**	**0.804**	**0.910**	**0.843**

Physical Parameter Estimation. We further evaluate the accuracy of estimated physical properties on our synthetic dataset, where the ground-truth Young's Modulus E^{gt} is available. We define the Material Accuracy (MA) metric as the percentage of particles where the estimated modulus E^{pred} falls within a tolerance threshold δ (set to 0.2):

$$\text{MA} = \frac{1}{P} \sum_{p=1}^{P} \mathbb{I} \left(\frac{|E_p^{\text{pred}} - E_p^{\text{gt}}|}{E_p^{\text{gt}}} \leq \delta \right) \tag{6}$$

The results are reported in Table 3. PhysInteract (Ours) achieves a high average accuracy of 84.3%, demonstrating that our method can reliably recover underlying physical properties from monocular video.

Figure 4: Visual comparison against baseline methods. We compare PhysInteract with PhysDreamer Zhang et al. (2024), DreamGaussian4D Ren et al. (2023), and GPT+PhysGaussian Xie et al. (2024a) on a real-world "toy rope" sequence. PhysDreamer generates distorted geometries due to the lack of explicit interaction modeling. DreamGaussian4D exhibits artifacts and a loss of structural coherence during large motions. GPT+PhysGaussian produces plausible but inaccurate motion dynamics due to incorrect material estimation. In contrast, PhysInteract (Ours) faithfully reconstructs the interaction dynamics, closely matching the Ground Truth.

4.3 Qualitative Analysis

Comparison with Baselines. Figure 3 and Figure 4 present visual comparisons. Baseline methods struggle to capture the causal relationship between interaction and deformation. For instance, in Scene 5 (Balloon
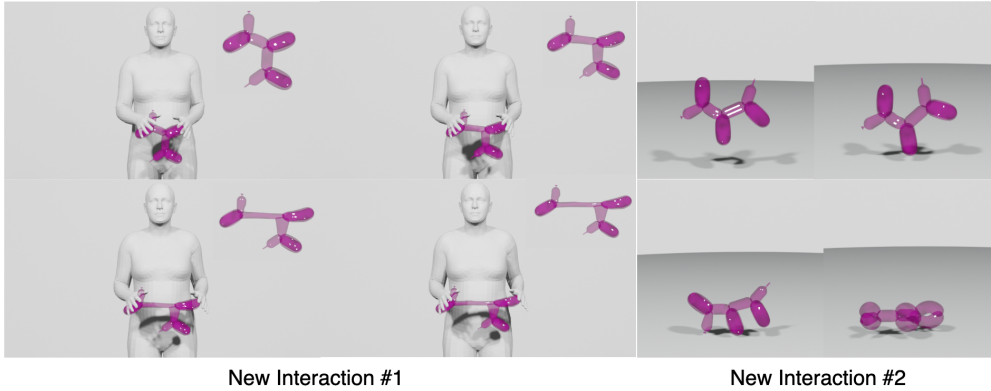
Figure 5: Generalization to novel interactions. Once the material field is learned from a reference video, PhysInteract enables *zero-shot* simulation of unseen interactions. Here, we apply two distinct new forces to the balloon dog (Top: pulling the leg; Bottom: compressing the body). The object responds with physically plausible elastic deformations, demonstrating that our method learns intrinsic physical properties rather than overfitting to the training video.

Dog), baselines fail to model the elastic rebound caused by the point interaction, whereas PhysInteract faithfully reconstructs the physical response.

Generalization to Novel Interactions. A key advantage of estimating intrinsic physical properties is the ability to generalize. As shown in Figure 5, once the material field is learned, PhysInteract can synthesize physically plausible dynamics under *novel, unseen interactions* (e.g., applying forces to different parts of the rope) without any re-training. This capability is unique to our physics-based formulation.

4.4 User Study

We conducted a user study with 50 participants to evaluate *Motion Realism (MR)* and *Visual Quality (VQ)* on a 5-point Likert scale. Methods were anonymized and presented in random order. Table 4 summarizes the results. PhysInteract significantly outperforms baselines, achieving an average MR of 4.3, compared to the second-best (DreamGaussian4D) at 3.6. This confirms that our physics-grounded approach aligns better with human perception of realistic interaction.

Table 4: User study results. Human ratings on Motion Realism (MR) and Visual Quality (VQ). Abbreviations: PD (PhysDreamer), DG4D (DreamGaussian4D), GPT-PG (GPT+PhysGaussian).

| Method	Scene 1		Scene 2		Scene 3		Scene 4		Scene 5		Scene 6	
	MR	VQ	MR	VQ	MR	VQ	MR	VQ	MR	VQ	MR	VQ
PD	1.8	2.0	1.5	1.7	2.2	2.5	1.9	2.1	2.0	2.3	1.6	1.9
DG4D	3.8	4.0	3.5	3.7	4.0	4.2	3.9	4.1	3.4	3.2	3.3	3.2
GPT-PG	3.9	4.1	3.6	3.8	4.1	4.3	3.8	4.0	3.1	2.9	3.2	2.8
Ours	**4.5**	**4.7**	**4.3**	**4.6**	**4.6**	**4.8**	**4.4**	**4.7**	**4.2**	**4.5**	**4.3**	**4.6**
Method	Scene 7		Scene 8		Scene 9		Scene 10		Scene 11		Average	
	MR	VQ	MR	VQ	MR	VQ	MR	VQ	MR	VQ	MR	VQ
PD	1.7	2.0	1.6	1.9	1.4	1.7	1.5	1.8	1.3	1.6	1.7	2.0
DG4D	3.9	4.1	3.7	3.9	3.4	3.6	3.5	3.7	3.3	3.5	3.6	3.8
GPT-PG	3.8	4.0	3.5	3.7	3.3	3.5	3.4	3.6	3.2	3.4	3.5	3.7
Ours	**4.4**	**4.6**	**4.2**	**4.5**	**4.0**	**4.3**	**4.1**	**4.4**	**3.9**	**4.2**	**4.3**	**4.5**
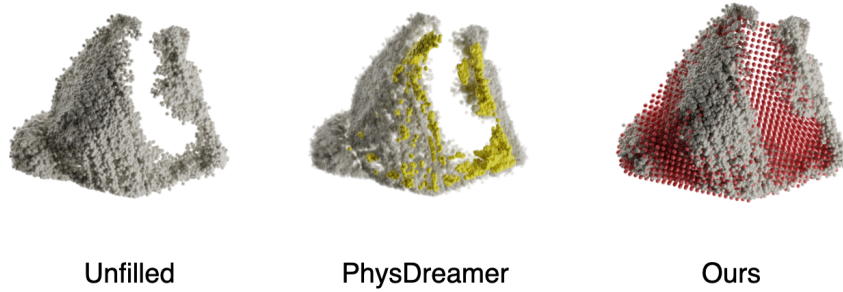
Figure 6: Ablation on internal filling strategy. We compare particle distributions for the simulation. (Left) Raw 3D Gaussians are too sparse for continuum mechanics. (Middle) PhysDreamer's mesh-based voxelization fails to capture the volume, resulting in structural holes (highlighted in yellow) that destabilize the simulation. (Right) Our approach, which densifies particles within Gaussian ellipsoids, produces a robust and dense continuum volume (red particles), ensuring stable and accurate physics simulation.

4.5 Ablation Study

Impact of joint optimization. A core contribution of PhysInteract is the joint optimization of both material properties and interaction trajectories. To validate this, we compare our full model against a variant (w/o JO) in which the interaction trajectory is fixed to the tracker's initialization and only material properties are optimized. As shown in the second row of Table 3, excluding trajectory optimization leads to a significant drop in material estimation accuracy (Avg. decreases from 0.843 to 0.715). This is because initial trajectories from vision trackers are often noisy; without refinement, the optimizer forces the material parameters to overfit these noisy trajectories, resulting in incorrect physical properties.

Effectiveness of Internal Filling. We validate our internal filling strategy by comparing it against the voxelization-based filling used in PhysDreamer. As visualized in Figure 6, converting sparse 3D Gaussians directly to mesh for voxelization often results in holes and artifacts. In contrast, our approachdensifies particles within Gaussian ellipsoids before fillingproduces a robust continuum representation, ensuring stable MPM simulation.

5 Conclusion and Limitations

Conclusion. In this work, we introduced PhysInteract, a unified framework for modeling physically plausible human-object interactions from monocular videos. By bridging the gap between 3D visual representations and differentiable physics simulation, PhysInteract addresses the critical challenge of inferring causal physical dynamics from purely visual observations. Our core innovation lies in the joint optimization strategy, which iteratively refines both the object's material properties and the interaction trajectories within a differentiable MPM solver. Extensive experiments on a curated dataset of synthetic and real-world scenarios demonstrate that PhysInteract significantly outperforms existing diffusion-based and kinematic approaches in terms of visual fidelity and motion realism. Furthermore, by recovering intrinsic physical parameters, our method enables zero-shot synthesis of dynamics under novel user-defined interactions, taking a significant step towards creating interactive and immersive virtual experiences.

Limitations. Despite its promising results, PhysInteract has several limitations that suggest avenues for future research. **(1)** Computational Complexity: while differentiable MPM ensures physical accuracy, it is computationally intensive compared to purely kinematic or generative methods. Optimizing a single sequence currently requires approximately 30 minutes, limiting its application in real-time scenarios. Future work could explore neural surrogates or reduced-order models to accelerate the simulation loop. **(2)** Dependence on 3D Initialization: our method relies on the quality of the initial static 3D representation (e.g., 3DGS). Severe occlusions or reconstruction artifacts in the initial 3D model can propagate errors into the physical simulation. Integrating dynamic 3D reconstruction jointly with physics optimization could mitigate this

issue. **(3)** Material Complexity: we model objects using a hyperelastic constitutive model suitable for a wide range of solids. However, modeling extremely complex materials (e.g., fluids, fracturing objects, or cloth with intricate weaving) remains a challenge. Extending our differentiable pipeline to support a broader library of constitutive models is a promising direction for future exploration.

References

Josh Achiam, Steven Adler, Sandhini Agarwal, Lama Ahmad, Ilge Akkaya, Florencia Leoni Aleman, Diogo Almeida, Janko Altenschmidt, Sam Altman, Shyamal Anadkat, et al. Gpt-4 technical report. arXiv preprint arXiv:2303.08774, 2023.

Sherwin Bahmani, Ivan Skorokhodov, Victor Rong, Gordon Wetzstein, Leonidas Guibas, Peter Wonka, Sergey Tulyakov, Jeong Joon Park, Andrea Tagliasacchi, and David B Lindell. 4d-fy: Text-to-4d generation using hybrid score distillation sampling. In Proceedings of the IEEE/CVF Conference on Computer Vision and Pattern Recognition, pp. 7996–8006, 2024.

Jinze Bai, Shuai Bai, Yunfei Chu, Zeyu Cui, Kai Dang, Xiaodong Deng, Yang Fan, Wenbin Ge, Yu Han, Fei Huang, et al. Qwen technical report. arXiv preprint arXiv:2309.16609, 2023.

Ce Chen, Shaoli Huang, Xuelin Chen, Guangyi Chen, Xiaoguang Han, Kun Zhang, and Mingming Gong. Ct4d: Consistent text-to-4d generation with animatable meshes. arXiv preprint arXiv:2408.08342, 2024a.

Xi Chen, Zhiheng Liu, Mengting Chen, Yutong Feng, Yu Liu, Yujun Shen, and Hengshuang Zhao. Livephoto: Real image animation with text-guided motion control. In European Conference on Computer Vision, pp. 475–491. Springer, 2024b.

Devikalyan Das, Christopher Wewer, Raza Yunus, Eddy Ilg, and Jan Eric Lenssen. Neural parametric gaussians for monocular non-rigid object reconstruction. In Proceedings of the IEEE/CVF Conference on Computer Vision and Pattern Recognition, pp. 10715–10725, 2024.

Yuanxing Duan, Fangyin Wei, Qiyu Dai, Yuhang He, Wenzheng Chen, and Baoquan Chen. 4d-rotor gaussian splatting: towards efficient novel view synthesis for dynamic scenes. In ACM SIGGRAPH 2024 Conference Papers, pp. 1–11, 2024.

Yutao Feng, Yintong Shang, Xuan Li, Tianjia Shao, Chenfanfu Jiang, and Yin Yang. Pie-nerf: Physics-based interactive elastodynamics with nerf. In Proceedings of the IEEE/CVF Conference on Computer Vision and Pattern Recognition, pp. 4450–4461, 2024.

Shubham Goel, Georgios Pavlakos, Jathushan Rajasegaran, Angjoo Kanazawa, and Jitendra Malik. Humans in 4d: Reconstructing and tracking humans with transformers. In Proceedings of the IEEE/CVF International Conference on Computer Vision, pp. 14783–14794, 2023.

Yuanming Hu. Taichi: An open-source computer graphics library. arXiv preprint arXiv:1804.09293, 2018.

Tianyu Huang, Haoze Zhang, Yihan Zeng, Zhilu Zhang, Hui Li, Wangmeng Zuo, and Rynson WH Lau. Dreamphysics: Learning physics-based 3d dynamics with video diffusion priors. In Proceedings of the AAAI Conference on Artificial Intelligence, volume 39, pp. 3733–3741, 2025.

Chenfanfu Jiang, Craig Schroeder, Joseph Teran, Alexey Stomakhin, and Andrew Selle. The material point method for simulating continuum materials. In Acm siggraph 2016 courses, pp. 1–52. 2016.

Yanqin Jiang, Li Zhang, Jin Gao, Weimin Hu, and Yao Yao. Consistent4d: Consistent 360 {\deg} dynamic object generation from monocular video. arXiv preprint arXiv:2311.02848, 2023.

Bernhard Kerbl, Georgios Kopanas, Thomas Leimkühler, and George Drettakis. 3d gaussian splatting for real-time radiance field rendering. ACM Trans. Graph., 42(4):139–1, 2023.

Agelos Kratimenos, Jiahui Lei, and Kostas Daniilidis. Dynmf: Neural motion factorization for real-time dynamic view synthesis with 3d gaussian splatting. In European Conference on Computer Vision, pp. 252–269. Springer, 2024.

Xuan Li, Yi-Ling Qiao, Peter Yichen Chen, Krishna Murthy Jatavallabhula, Ming Lin, Chenfanfu Jiang, and Chuang Gan. Pac-nerf: Physics augmented continuum neural radiance fields for geometry-agnostic system identification. arXiv preprint arXiv:2303.05512, 2023.

Zhengqi Li, Richard Tucker, Noah Snavely, and Aleksander Holynski. Generative image dynamics. In Proceedings of the IEEE/CVF Conference on Computer Vision and Pattern Recognition, pp. 24142–24153, 2024.

Yiqing Liang, Numair Khan, Zhengqin Li, Thu Nguyen-Phuoc, Douglas Lanman, James Tompkin, and Lei Xiao. Gaufre: Gaussian deformation fields for real-time dynamic novel view synthesis. In 2025 IEEE/CVF Winter Conference on Applications of Computer Vision (WACV), pp. 2642–2652. IEEE, 2025.

Jiajing Lin, Zhenzhong Wang, Dejun Xu, Shu Jiang, Yunpeng Gong, and Min Jiang. Phys4dgen: Physics-compliant 4d generation with multi-material composition perception. In Proceedings of the 33rd ACM International Conference on Multimedia, pp. 10398–10407, 2025.

Youtian Lin, Zuozhuo Dai, Siyu Zhu, and Yao Yao. Gaussian-flow: 4d reconstruction with dynamic 3d gaussian particle. In Proceedings of the IEEE/CVF Conference on Computer Vision and Pattern Recognition, pp. 21136–21145, 2024.

Huan Ling, Seung Wook Kim, Antonio Torralba, Sanja Fidler, and Karsten Kreis. Align your gaussians: Text-to-4d with dynamic 3d gaussians and composed diffusion models. In Proceedings of the IEEE/CVF conference on computer vision and pattern recognition, pp. 8576–8588, 2024.

Fangfu Liu, Hanyang Wang, Shunyu Yao, Shengjun Zhang, Jie Zhou, and Yueqi Duan. Physics3d: Learning physical properties of 3d gaussians via video diffusion. arXiv preprint arXiv:2406.04338, 2024a.

Shilong Liu, Zhaoyang Zeng, Tianhe Ren, Feng Li, Hao Zhang, Jie Yang, Qing Jiang, Chunyuan Li, Jianwei Yang, Hang Su, et al. Grounding dino: Marrying dino with grounded pre-training for open-set object detection. In European conference on computer vision, pp. 38–55. Springer, 2024b.

Ilya Loshchilov and Frank Hutter. Decoupled weight decay regularization. arXiv preprint arXiv:1711.05101, 2017.

Zijie Pan, Zeyu Yang, Xiatian Zhu, and Li Zhang. Efficient4d: Fast dynamic 3d object generation from a single-view video. arXiv preprint arXiv:2401.08742, 2024.

Ben Poole, Ajay Jain, Jonathan T Barron, and Ben Mildenhall. Dreamfusion: Text-to-3d using 2d diffusion. arXiv preprint arXiv:2209.14988, 2022.

Alec Radford, Karthik Narasimhan, Tim Salimans, Ilya Sutskever, et al. Improving language understanding by generative pre-training. 2018.

Nikhila Ravi, Valentin Gabeur, Yuan-Ting Hu, Ronghang Hu, Chaitanya Ryali, Tengyu Ma, Haitham Khedr, Roman Rädle, Chloe Rolland, Laura Gustafson, et al. Sam 2: Segment anything in images and videos. arXiv preprint arXiv:2408.00714, 2024.

Jiawei Ren, Liang Pan, Jiaxiang Tang, Chi Zhang, Ang Cao, Gang Zeng, and Ziwei Liu. Dreamgaussian4d: Generative 4d gaussian splatting. arXiv preprint arXiv:2312.17142, 2023.

Uriel Singer, Shelly Sheynin, Adam Polyak, Oron Ashual, Iurii Makarov, Filippos Kokkinos, Naman Goyal, Andrea Vedaldi, Devi Parikh, Justin Johnson, et al. Text-to-4d dynamic scene generation. arXiv preprint arXiv:2301.11280, 2023.

Qi Sun, Zhiyang Guo, Ziyu Wan, Jing Nathan Yan, Shengming Yin, Wengang Zhou, Jing Liao, and Houqiang Li. Eg4d: Explicit generation of 4d object without score distillation. arXiv preprint arXiv:2405.18132, 2024.

Xiyang Tan, Ying Jiang, Xuan Li, Zeshun Zong, Tianyi Xie, Yin Yang, and Chenfanfu Jiang. Physmotion: Physics-grounded dynamics from a single image. arXiv preprint arXiv:2411.17189, 2024.

Bo Wang, Jian Li, Yang Yu, Li Liu, Zhenping Sun, and Dewen Hu. Scenetracker: Long-term scene flow estimation network. IEEE Transactions on Pattern Analysis and Machine Intelligence, 2025.

Zhou Wang, Alan C Bovik, Hamid R Sheikh, and Eero P Simoncelli. Image quality assessment: from error visibility to structural similarity. IEEE transactions on image processing, 13(4):600–612, 2004.

Tianyi Xie, Zeshun Zong, Yuxing Qiu, Xuan Li, Yutao Feng, Yin Yang, and Chenfanfu Jiang. Physgaussian: Physics-integrated 3d gaussians for generative dynamics. In Proceedings of the IEEE/CVF Conference on Computer Vision and Pattern Recognition, pp. 4389–4398, 2024a.

Yiming Xie, Chun-Han Yao, Vikram Voleti, Huaizu Jiang, and Varun Jampani. Sv4d: Dynamic 3d content generation with multi-frame and multi-view consistency. arXiv preprint arXiv:2407.17470, 2024b.

Gengshan Yang, Deqing Sun, Varun Jampani, Daniel Vlasic, Forrester Cole, Huiwen Chang, Deva Ramanan, William T Freeman, and Ce Liu. Lasr: Learning articulated shape reconstruction from a monocular video. In Proceedings of the IEEE/CVF Conference on Computer Vision and Pattern Recognition, pp. 15980–15989, 2021.

Zeyu Yang, Zijie Pan, Chun Gu, and Li Zhang. Diffusion⊖2: Dynamic 3d content generation via score composition of video and multi-view diffusion models. arXiv preprint arXiv:2404.02148, 2024.

Yuyang Yin, Dejia Xu, Zhangyang Wang, Yao Zhao, and Yunchao Wei. 4dgen: Grounded 4d content generation with spatial-temporal consistency. arXiv preprint arXiv:2312.17225, 2023.

Yifei Zeng, Yanqin Jiang, Siyu Zhu, Yuanxun Lu, Youtian Lin, Hao Zhu, Weiming Hu, Xun Cao, and Yao Yao. Stag4d: Spatial-temporal anchored generative 4d gaussians. In European Conference on Computer Vision, pp. 163–179. Springer, 2024.

Shiwei Zhang, Jiayu Wang, Yingya Zhang, Kang Zhao, Hangjie Yuan, Zhiwu Qin, Xiang Wang, Deli Zhao, and Jingren Zhou. I2vgen-xl: High-quality image-to-video synthesis via cascaded diffusion models. arXiv preprint arXiv:2311.04145, 2023.

Tianyuan Zhang, Hong-Xing Yu, Rundi Wu, Brandon Y Feng, Changxi Zheng, Noah Snavely, Jiajun Wu, and William T Freeman. Physdreamer: Physics-based interaction with 3d objects via video generation. In European Conference on Computer Vision, pp. 388–406. Springer, 2024.

Haoyu Zhao, Hao Wang, Xingyue Zhao, Hao Fei, Hongqiu Wang, Chengjiang Long, and Hua Zou. Efficient physics simulation for 3d scenes via mllm-guided gaussian splatting. arXiv preprint arXiv:2411.12789, 2024.

Yuyang Zhao, Zhiwen Yan, Enze Xie, Lanqing Hong, Zhenguo Li, and Gim Hee Lee. Animate124: Animating one image to 4d dynamic scene. arXiv preprint arXiv:2311.14603, 2023.